3D Seismic Imaging – Another Look at Scaling and Resolution

B. Milkereit[1], E. Adam[2] and T. Bohlen[3]; [1] University of Toronto, Dept. of Physics, Toronto, Canada M5S 1A7; [2] Hydro-Quebec, Quebec City, Canada; [3] Kiel University, Geosciences, Germany

Abstract

3D surface seismic and multi-offset vertical seismic profiling (VSP) techniques can be employed to image target zones (such as hydrocarbon reservoirs and massive sulphide orebodies) in complex geological settings. The integration of petrophysical data and 3D elastic modeling studies provide new insights in the scale dependent petrophysical parameters and the internal structure of the target zone. Forward modeling studies demonstrate that directional scattering and wavefront healing place important constraints on how we handle static corrections and azimuth binning in 3D seismic datasets.

Introduction

The effects of heterogeneities on seismic wave propagation can be described in terms of different propagation regimes (Wu, 1989): quasi-homogeneous for heterogeneities too small to be seen by seismic waves, Rayleigh scattering, Mie scattering and small-angle scattering. These scattering regimes cause characteristic amplitude, phase and travel time fluctuation, which can be used to obtain estimates of scale length and thereby assess lateral continuity of lithological units and structure in the immediate vicinity of boreholes. Horizontal resolution of exploration seismic data is often discussed in terms of Fresnel zone. For surface and VSP data, the Fresnel radius increases with increasing depth of investigation. In addition, the lateral resolution is limited by the effective frequency content of the seismic signal. Here we present 3-D elastic modeling results for VSP and 3D surface seismic studies. Forward modeling is based on the implementation of 3D elastic FD codes on massive parallel and/or distributed computing resources using MPI (message passing interface). For parallelization the 3D model is decomposed into subvolumes. Each processing element (PE) or CPU is updating the wavefield within its portion of the grid. For wavefield update we apply staggered-grid velocity-stress finite difference equations which are of 4th order accuracy in space and of second order accuracy in time (Robertsson et al., 1994). The processors lying at top of the global grid apply a free surface boundary condition while the processors at the edges of the model apply an absorbing boundary condition. At the internal edges the processors exchange wavefield information. By clustering conventional PCs, wall clock time for 3D FD modeling can be significantly reduced and the possible grid sizes significantly increased (Bohlen and Milkereit, 2001; Bohlen et al., 2003).

Methodology and Objectives

In heterogeneous media, the angular and frequency dependent seismic responses point towards unique statistical distributions of physical properties in a reservoir zone. Investigations of the statistical nature of velocity and density perturbations provided useful insights into mechanisms governing wave propagation as there exists a strong correlation between the spatial properties of the velocity field of a reflective target and the lateral correlation length of the resulting seismic wave field. Synthetic examples of waveform data from two forward scattering/transmission 3D seismic experiments are shown in Figure 1.
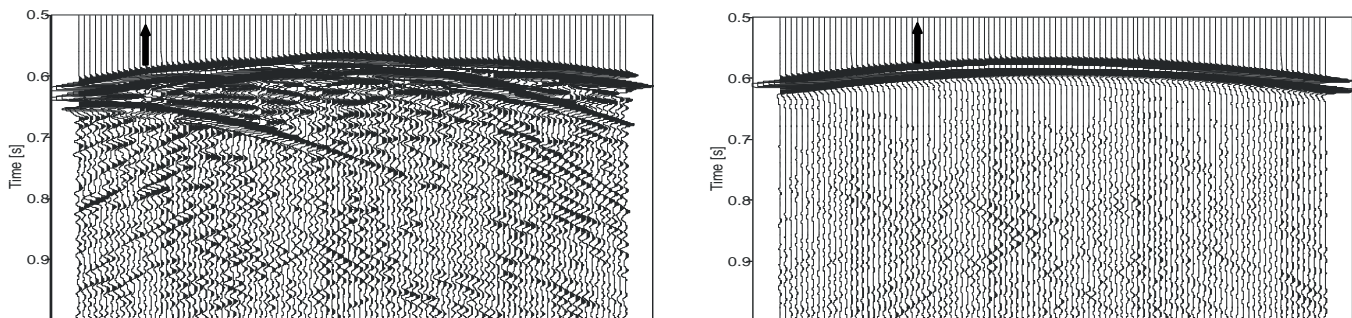

Figure 1: FD modeling of transmitted wavefield through heterogeneous medium with random fluctuations of elastic parameters. a) Fluctuation of elastic moduli and density; b) fluctuation of density only. Arrows indicate propagation direction.

3D Elastic Seismic-Wave Scattering

Based on the petrophysical data, many hydrocarbon reservoirs and sulfide ores should make strong P-wave, S-wave and converted wave reflectors against most background velocity models. In the context of realistic geological models, 3D numerical simulations are required to better assess elastic wave interactions with high seismic impedance targets. Here we study the influence of composition and shape of seismic high impedance targets on the full scattered wavefield through a series of numerical modeling experiments based on the 3D elastic finite-difference (FD) method. For example, massive sulfide ores consisting of the end-member sulfide minerals pyrite, sphalerite, and galena, which span the full range of observed P- and S- wave velocities and densities in ore rocks, as well as gabbro inclusions, are investigated for different shapes which represent the complex morphologies often observed for ore deposits. 3D FD modeling revealed that large ore deposits lead to a strong and complex scattering response that is often dominated by shear-wave events (Bohlen et al., 2003).
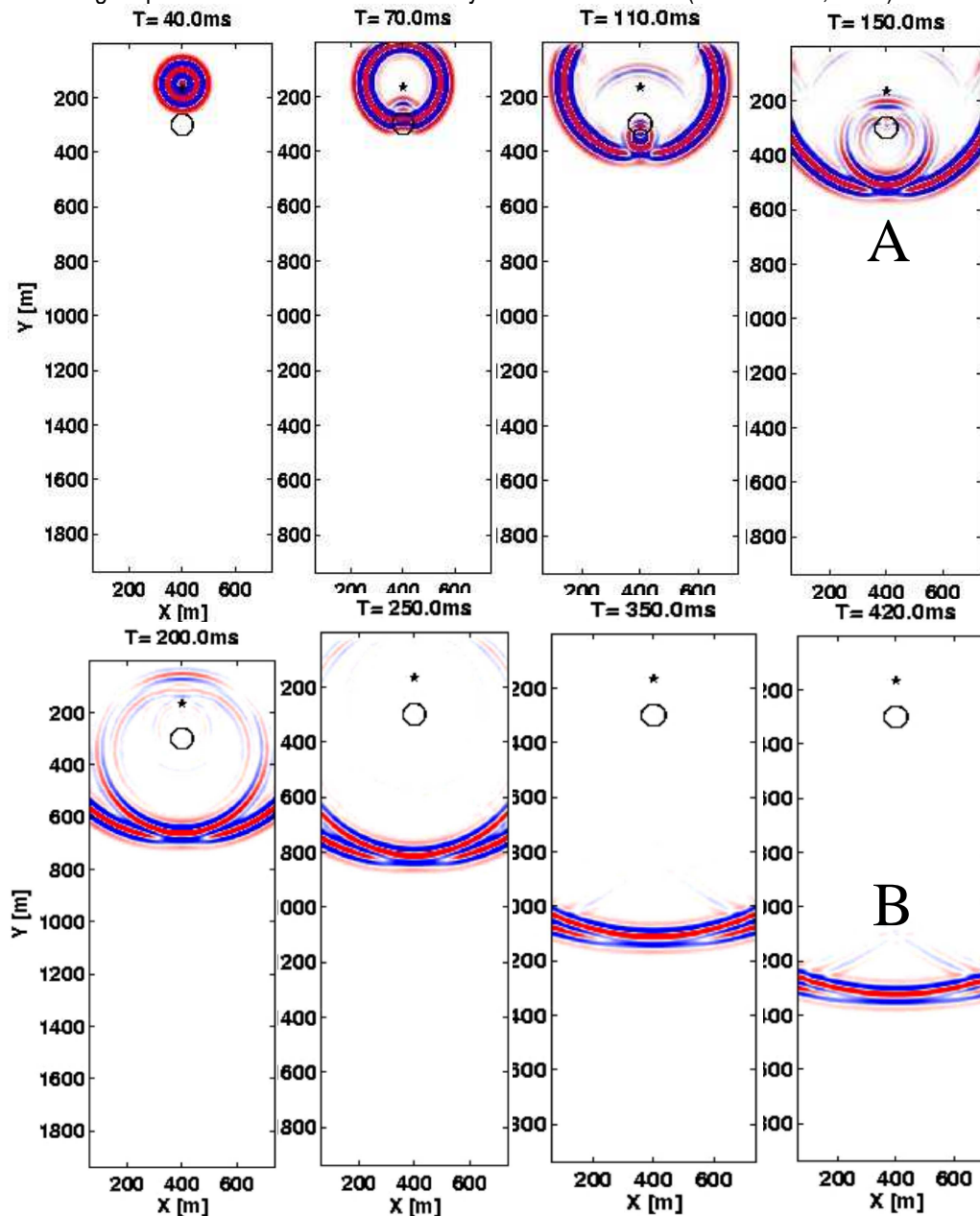

Fig 2. Finite-difference snapshots of forward and backward scattered compressional waves for a high impedance contrast, low P-wave velocity sphere in a homogeneous background. Note scattering coda generated by the sphere and significant travel time delays for the direct (forward scattered) wavefield (marked A). At late times, the direct wave "heals" (marked B).

Consequences I (Wavefront Healing): 3D Static Corrections

Tomographic traveltime inversion studies (Dahlen, 2002) suggests that time delays observed in the seismic wavefield are caused by heterogeneities that are close to the receivers. Heterogeneities that are far from the receiver do not affect the seismic arrivals as the waves "heal" quite rapidly. These observations are opening the way to fast and accurate methods of estimating refraction static correction. Based on wavefield healing, a new approach that combines the accuracy of the generalized linear inversion of first break pick times has been developed (Hampson and Russell, 1984). Taken into account wavefront healing, the method that we propose simplifies the refraction static correction problem by solving the shot and receiver static corrections independently. We first estimate the short wavelength component of the static correction while the long wavelength component is attributed to the refractor velocity variations. Finally, with the short wavelength shot and receiver statics in place, we solve for a smooth bedrock velocity model. This simple and fast method was applied to a 3-D survey acquired for base metal exploration that consist of about 1000 shot points recorded by up to 1983 receivers (Milkereit et al., 2000). In the survey area near surface conditions and data quality are highly variable making first break picking difficult.

Consequences II (Directional Scattering): 3D Seismic Imaging

3D seismic data acquisition and processing must capture and preserve the scattering response from a local high impedance targets, such as a deep massive sulfide deposit. As indicated by 3D elastic wave modeling studies, amplitude anomalies will often be recorded down-dip of the deposit. In addition, the amplitude anomalies are often restricted to a relatively small range of azimuths. At the same time, reflective target stratigraphy of the host geological environment must be imaged. 3D shot-receiver geometries for equivalent offset prestack time migration (Bancroft et al., 1998) are shown in Figure 3.
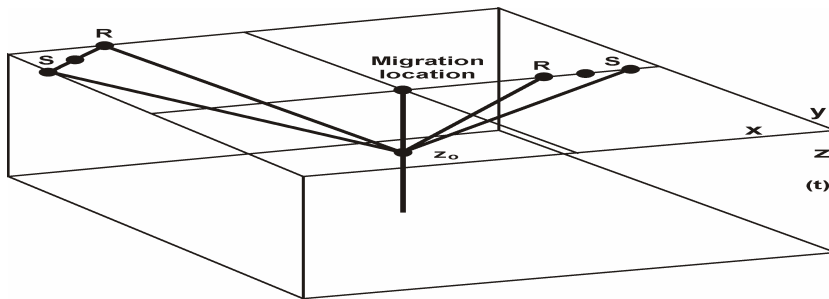

Fig. 3. 3D seismic acquisition geometry for prestack migration. All source-receiver contributions are sorted by equivalent offset and azimuth (in respect to subsurface structure).

This approach allows the sorting and binning for a range of offsets and azimuths. Equivalent offset gathers (before stack) from the Matagami 3D seismic survey area are shown in Fig. 4 (Adam et al., 2003). The panel on the right shows the seismic reflection response from the steeply-dipping target stratigraphy (preferred azimuth range: 300^0-360^0). The response from the massive sulfides (indicated by arrow in Fig.4, left panel) is best seen by a different azimuth range (120^0-180^0). This example shows that special care must be taken to preserve the seismic response of a complex massive sulfide deposit. Conventional 3D binning and stacking may easily attenuate the target response.
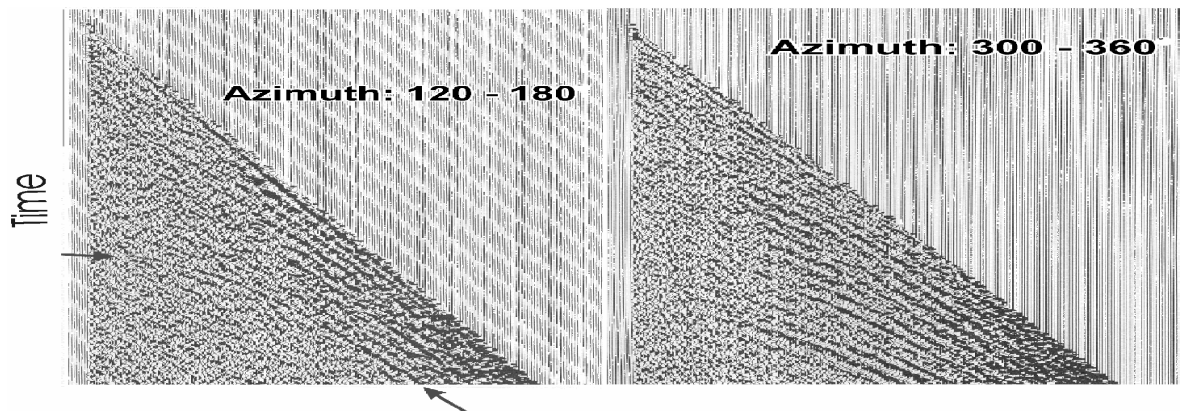

Fig. 4 Equivalent offset gathers for three different azimuths from the Matagami 3D seismic data set (Adam et al., 2003). Reflections from target stratigraphy are best imaged in right panel. Note that the reflection from massive sulfides (left panel) requires a different azimuthal coverage.

Evolving Geophysics Through Innovation

True amplitude processing

Petrophysical data and 3D elastic modeling studies predict that many massive sulfide deposits should produce local "bright spot" reflection/diffraction amplitudes. In a low signal-to-noise environment, partial prestack migration techniques (such as the equivalent offset migration) can be used to preserve relative amplitudes throughout the 3D seismic data processing sequence. Figure 5 shows a cross-line from a 3D seismic data set acquired across the Sudbury basin, one of the richest nickel-producing areas in the world (Milkereit et al., 2000). Massive sulfide deposits are located at the footwall contact of the Sudbury Igneous Complex (SIC). The trace envelope display highlights the local "bright spot" anomalies (right panel). The trace envelope display is ideally suited for volume rendering, integration of borehole geophysical data, and 3D visualization of seismic, drill-hole and surface geological data.
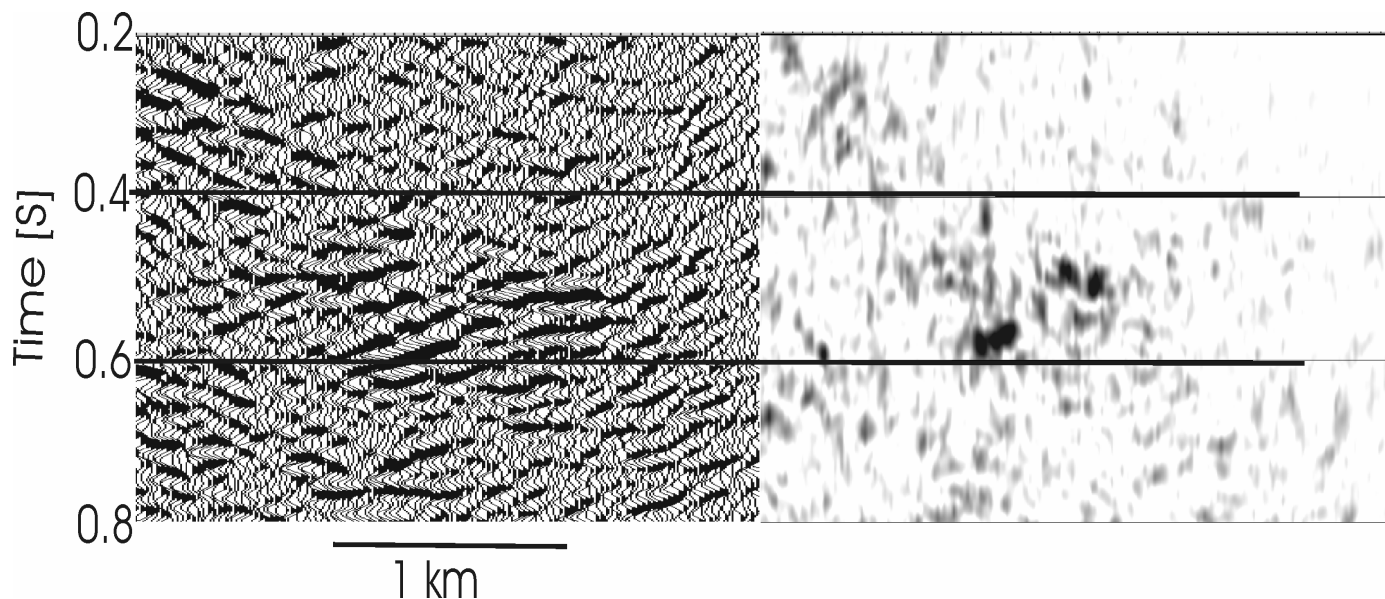

Fig. 5. True amplitude 3D prestack migrated data from the Sudbury Basin. Left: conventional seismic display of a cross-line section; Right: Trace envelope display to highlight "bright spot" reflection within target stratigraphy.

References

Adam E., G. Perron , G. Arnold , L. Matthews and B. Milkereit, 3-D seismic imaging for VMS deposit exploration, Matagami, Quebec, in: Hardrock Seismic Exploration, SEG, Tulsa, 239-258, 2003.

Bancroft, J.C., Geiger, H.D., and Margrave, G.F., The equivalent offset method of prestack time migration, geophysics, 63, 2041-2053, 1998.

Bohlen, T., C. Müller and B. Milkereit, Elastic seismic wave scattering from massive sulfide orebodies: On the role of composition and shape, in: Hardrock Seismic Exploration, SEG, Tulsa, 86-102, 2003.

Bohlen, T. and Milkereit, B., Parallel 3-D viscoelastic finite-difference seismic modeling, EAGE 63rd Conference & Exhibition, Amsterdam, The Netherlands, Expanded Abstract, 2001.

Dahlen, F.A., Bananas, Doughnuts and Seismic Traveltimes. Eos Trans. AGU, 83 (47), Fall Meeting Suppl., 2002.

Hampson, D. and Russell, B., First-break interpretation using generalized linear inversion: J. Can. Soc. Expl. Geophys., 20, No. 1, 40-54, 1984.

Milkereit, B., Berrer, E.K., King, A.R., Watts, A.H., Roberts, B., Adam, E., Eaton, D.W., Wu, J., and Salisbury, M., Development of 3-D seismic exploration technology for deep nickel-copper deposits - a case history from the Sudbury basin, Canada, Geophysics, 65, 1890-1899, 2000.

Robertsson, J.O.A., Blanch, J.O. and Symes, W.W, Viscoelastic Finite-Difference Modeling, Geophysics, 59, 1444-1456, 1994.

Wu, R.J., Seismic wave scattering, in: Solid Earth Geophysics, Editor: D.E. James, 1166-1187, 1989.